Supplementary Information

Revealing Thermodynamics of Individual Catalytic Steps based on Temperature-Dependent Single-Particle Nanocatalysis

Xiaodong Liu[a,b], Tao Chen[a], Weilin Xu[a,b*]

[a]State Key Laboratory of Electroanalytical Chemistry, & Jilin Province Key Laboratory of Low Carbon Chemical Power, Changchun Institute of Applied Chemistry, Chinese Academy of Science, 5625 Renmin Street, Changchun 130022, P.R. China.

[b]University of Science and Technology of China, Anhui 230026, China;

Fabrication of temperature-controllable flow cell

A quartz slide and a borosilicate coverslip (Gold Seal) was sealed up by 5-minute epoxy adhesive (Devcon) to make a space, which was separated by a modified double-sided tapes (3M) and epoxy adhesive into two rooms, the inner room (100 μm (height)×2 cm (length)×5 mm (width)) is the place where reaction takes place and the outer room is for the flow of water bath to control the temperature of the cell. Four holes were drilled on the quartz slide and connected with polyethylene tubings (Instech Laboratories, 0.076mm ID). A syringe pump (Harvard Apparatus) to make the inner solution continuous flow at the rate of 10 μL/min, and a peristaltic pump (Harvard Apparatus) to make the outer water continuous flow at the rate of 30 mL/min. The outer water was heated by a water bath and the thermocouple probe was stuck on the coverslip close to the inner room. 100 μL of Pt-nanoparticles solution was dropped onto quartz slide, and kept for 40min and then rinsed with amount of MilliQ water to remove unbound nanoparticles before the two rooms were formed on the quartz slide. The edges of the coverslip were sealed by 5 minute-epoxy (Devcon) after the rooms were made up.

Single-molecule reaction experiments

Single-molecule fluorescence measurements were performed on a homebuilt prism-type total internal reflection (TIR) fluorescence microscope based on an Olympus IX71 inverted microscope. A continuous wave circularly polarized 532 nm laser beam (CrystaLaser, GCL-025-L-0.5%) of 4-5mW was focused onto an area of ~80×80 μm^2 on the sample to directly excite the fluorescence of product, which was collected by a 60X NA1.2 water-immersion objective (UPLSAPO60XW, Olympus). The fluorescence of resorufin was filtered by filters (HQ550LP, HQ580m60), and projected onto a camera (AndoriXon EMCCD, DU-897U-CS0-#BV), which was controlled by an Andor IQ software. All optical filters are from Chroma Technology Corp. At the same area, a series of movies was collected at four temperatures (25 ^oC, 30 ^oC, 35 ^oC, 40 ^oC) with 0.1/frame. The movies are analyzed using a home-written IDL program, which can extract the fluorescence intensity trajectories from localized fluorescence spots individually across the entire movie. The intensity of each bright spot in an image is obtained by integrating the signal counts over an area of ~1×1 μm^2.

Synthesis and characterization of Pt nanoparticles

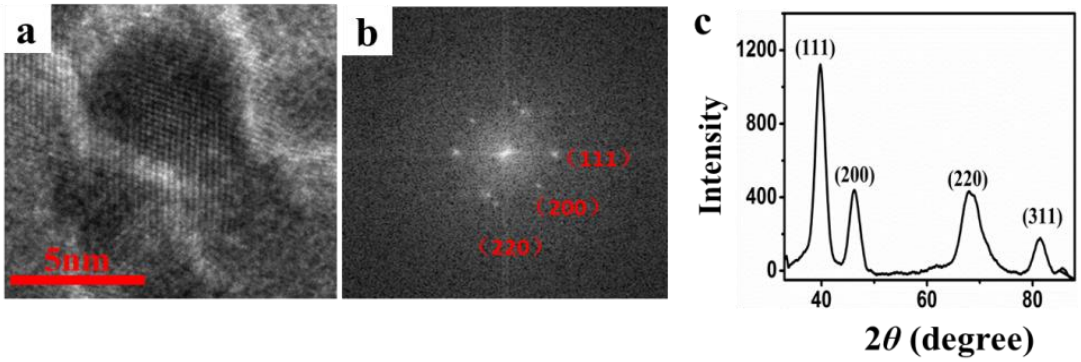

Figure S1. (a) High-resolution micrograph of Pt nanoparticles. (b) The corresponding FFT (fast Fourier transition) pattern from (a). (c) XRD characterization of Pt nanoparticles.

Ensemble measurements of Pt-nanoparticles catalyzed reaction

We tested the ability of the Pt-nanoparticle in catalyzing the reduction of resazurin to resorufin by hydrogen in ensemble measurements. The control experiments show there is no reduction reaction between resazurin and hydrogen without Pt nanoparticle, and there is no reaction between resazurin and Pt nanoparticle without hydrogen. After addition of hydrogen to the reaction solution containing resazurin and Pt nanoparticle, the color of solution turns from blue (resazurin) to red (resorufin) gradually. The experiments were carried out in water at four different temperatures and the catalytic reaction proceeded was monitored by UV-Vis absorption. The absorption spectrum of the reaction system shows a decrease of the resazurin absorption at 601 nm over time and an increase of the resorufin at 571 nm (Figure S2). The time profiles of the absorbance at 571 nm and 601 nm show the quantitative conversion of resazurin to resozufin catalyzed by Pt-nanoparticle (Figure S2 b, c, f). The rate of resazurin reduction reaction increases with the rising of temperature (Figure S3 a, b): with the same concentration of resazurin and Pt nanoparticle.

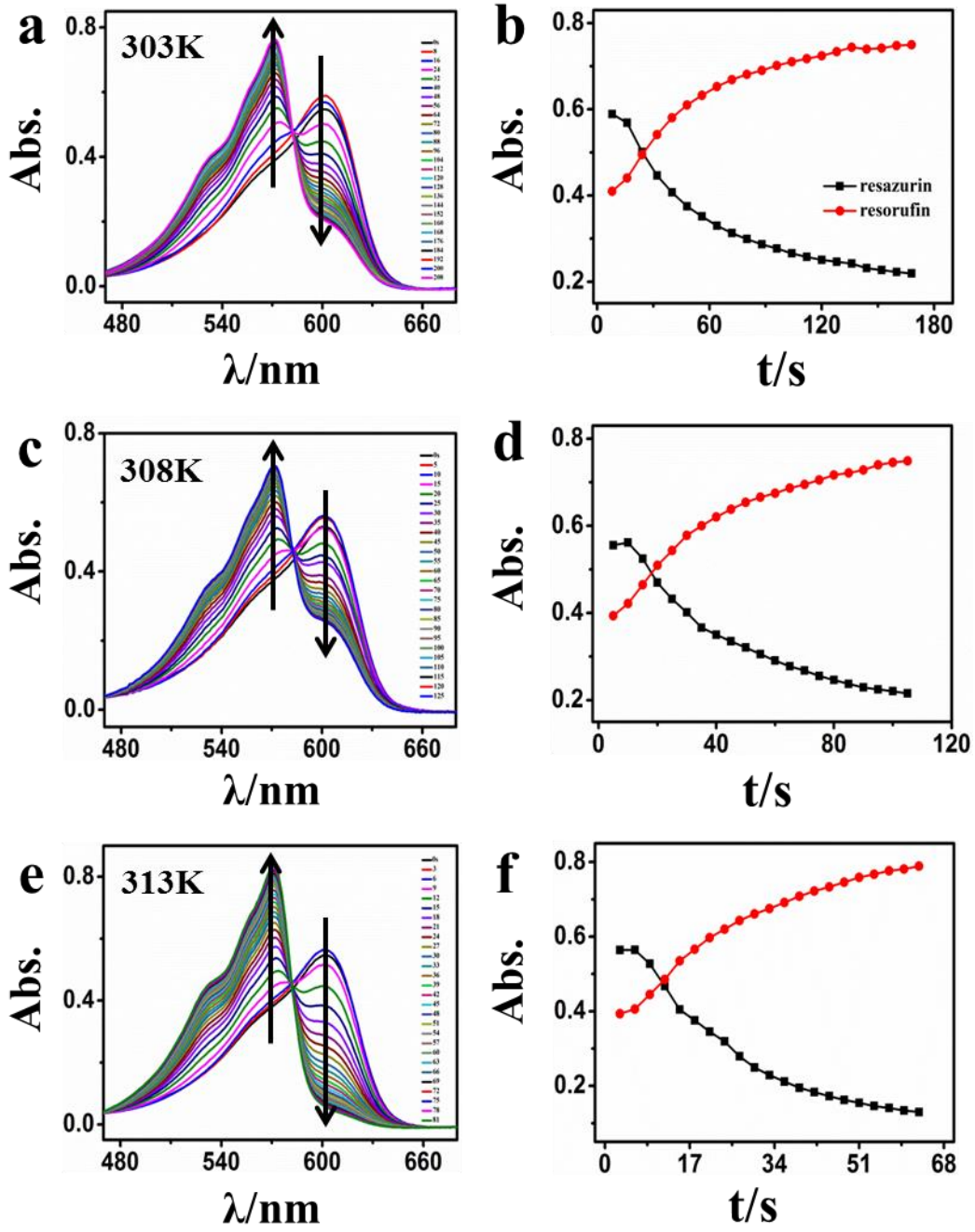

Figure S2. In situ absorption measurements of resazurin reduction by H_2 catalyzed by Pt-nanoparticles at different temperatures (a) 30 ^{o}C, (c) 35 ^{o}C and (e) 40 ^{o}C in aqueous solution. (b), (d) and (f) are the time profiles of absorbance at 601 and 571 nm from (a), (c), and (e), respectively.

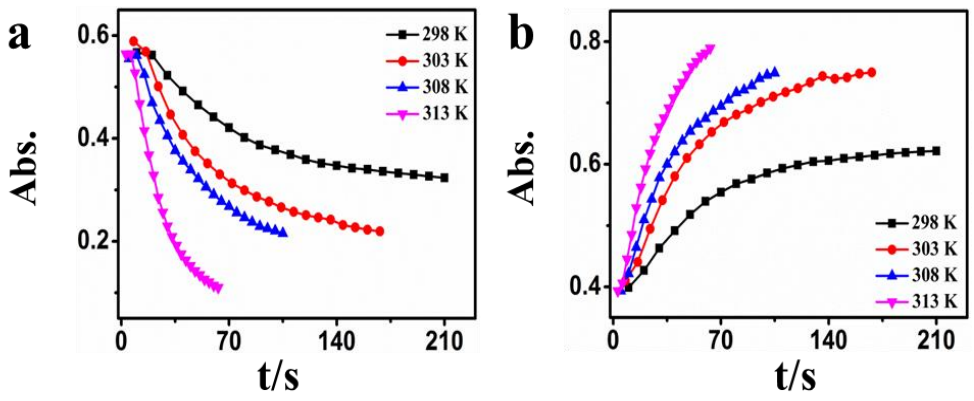

Figure S3. Time profiles of absorbance at 601 nm (a) and 571 nm (b) from Figure S1.

The fabrication of temperature-controllable experimental setup

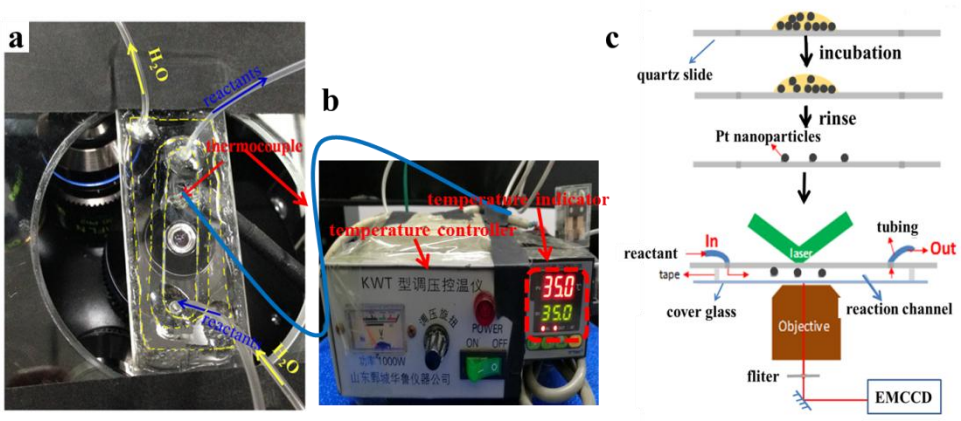

Scheme S1. (a) Photograph of a temperature-controllable microflow reaction cell equipped with a water bath. (b) The temperature-controllable equipment and temperature indicating device connecting with the reaction microflow cell by thermocouple. (c) Scheme for the fabrication of the microflow cell for single-molecule chemical reaction studies.

The kinetic mechanism for Pt nanoparticle catalyst

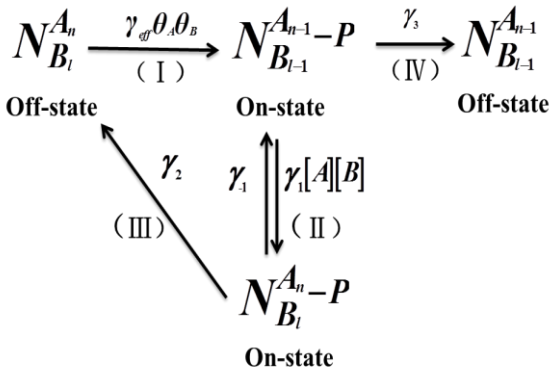

Scheme S2 The kinetic mechanism for the catalytic reduction reaction by Pt nanoparticle based on the Langmuir adsorption isotherm. *N*, Pt-nanoparticle; A, B, and *P* represent hydrogen, Resazurin, and Resorufin molecules; *n*, *l*, the number of H_2 and Resazurin molecules adsorbed on one nanoparticle surface at equilibrium; γ_{eff} the effective rate constant for the product formation process; γ_i the rate constants for

product dissociation steps; θ_A, θ_B, the fraction of catalytic sites occupied by hydrogen and Resazurin.

Derivation of the distribution of the off-time $f_{off}(\tau)$, and of $\langle \tau_{off} \rangle^{-1}$

A single-turnover trajectory consists of the product formation process (τ_{off}) and the product desorption process (τ_{on}). To analyze the statistical properties of τ_{off}, we considered the Langmuir-Hinshelwood mechanism for heterogeneous catalysis to analyze the reaction kinetics.[S3] The mechanism assumes that the two reactants binds on each nanoparticle surface are uniform and reversible at a fast adsorption equilibrium. And the adsorption of substrate molecules on nanoparticles is governed by the Langmuir adsorption isotherm.[S4] According to this mechanism, the kinetic scheme of product formation process that involves two reaction molecules is:

$$\underset{\textbf{Off-state}}{N_{B_l}^{A_n}} \xrightarrow{\gamma_{\textbf{eff}}} \underset{\textbf{On-state}}{N_{B_{l-1}}^{A_{n-1}}-P} \qquad (\text{I})$$

where *N* stands for the Pt nanoparticle, *A*, *B* represent substrate hydrogen and resazurin, respectively; *n*, *l* are the numbers of substrate molecules adsorbed on the nanoparticle surface at equilibrium; *P* is the product resorufin; γ_{eff} is the apparent rate constant for forming one product on one nanoparticle surface and takes the form:

$$\gamma_{app} = \gamma n_A n_B = \gamma n_T^2 \theta_A \qquad \text{(S1)}$$

where γ is the rate constant representing the intrinsic reactivity per catalytic site for the catalytic conversion reaction; n_A and n_B are the numbers of A and B molecule adsorbed at the catalytic site on one nanoparticle surface; n_T is the total number of the surface catalytic sites on one nanoparticle; θ_A, θ_B is the fraction of the occupied surface catalytic sites by substrates. Form the Langmuir adsorption isotherm:

$$n_A = n_T \theta_A = n_T \frac{\alpha_A[A]}{1+\alpha_A[A]+\alpha_B[B]} \qquad \text{(S2)}$$

$$n_B = n_T \theta_B = n_T \frac{\alpha_B[B]}{1+\alpha_A[A]+\alpha_B[B]} \qquad \text{(S3)}$$

Here α_A, α_B are the H_2 and resazurin adsorption-equilibrium constants, then we get

$$\gamma_{app} = \gamma n_T^2 \frac{\alpha_A[A]\alpha_B[B]}{(1+\alpha_A[A]+\alpha_B[B])^2} \qquad \text{(S4)}$$

In conventional ensemble measurements where the catalysis by a large of nano- particles are measured in solution, and the kinetic rate equations are:

$$\frac{d\left[N_{B_l}^{A_n}\right]}{d\tau} = -\gamma_{app}\left[N_{B_l}^{A_n}\right] \qquad \text{(S5)}$$

$$\frac{d\left[N_{B_{l-1}}^{A_{n-1}}\right]}{d\tau} = \gamma_{app}\left[N_{B_l}^{A_n}\right] \qquad \text{(S6)}$$

where $\left[N_{B_l}^{A_n}\right]$ is the concentration of Pt nanoparticles carrying no product, and $\left[N_{B_{l-1}}^{A_{n-1}}\right]$ is the concentration of nanoparticles on which one product molecule is generated.

Under the condition of single-nanoparticle measurements, the concentration of one nanoparticle is replaced by the probability of the single nanoparticle. Then the equations turn to:

$$\frac{dP_{\left[N_{B_l}^{A_n}\right]}(\tau)}{d\tau} = -\gamma_{app} P_{\left[N_{B_l}^{A_n}\right]}(\tau) \qquad \text{(S7)}$$

$$\frac{dP_{\left[N_{B_{l-1}}^{A_{n-1}}-P\right]}(\tau)}{d\tau} = \gamma_{app} P_{\left[N_{B_l}^{A_n}\right]}(\tau) \qquad \text{(S8)}$$

Where *P*(t)'s are the probabilities for finding the single nanoparticle in the state $N_{B_l}^{A_n}$ and $N_{B_l-1}^{A_{n-1}} - P$. In the

start of each τ_{off} reaction (t=0), no product molecule has formed. So under the initial conditions the equation are $P_{\left[N_{B_l}^{A_n}\right]}(\tau) = 1$, $P_{\left[N_{B_{l-1}}^{A_{n-1}}-P\right]}(\tau) = 0$. And at any time within τ_{off}, $P_{\left[N_{B_l}^{A_n}\right]}(\tau) + P_{\left[N_{B_{l-1}}^{A_{n-1}}-P\right]}(\tau) = 1$

We can then evaluate the probability density of the time $\Delta\tau$ needed to complete the off-time reaction, $f_{off}(\tau)$, that is, the probability density is τ_{off}. The probability for finding a particle τ is $f_{off}(\tau)\Delta\tau$, which is equal to the probability of switching from the $N_{B_l}^{A_n}$ state to the $N_{B_l-1}^{A_{n-1}} - P$ state for the nanoparticle between t=τ and t = $\tau + \Delta\tau$. In the limit of infinitesimal $\Delta\tau$, we obtain:

$$f_{off}(\tau) = \frac{dP_{\left[N_{B_{l-1}}^{A_{n-1}}-P\right]}(\tau)}{d\tau} = \gamma_{app} P_{\left[N_{B_l}^{A_n}\right]}(\tau) = \gamma n_T^2 \frac{\alpha_A[A]\alpha_B[B]}{(1+\alpha_A[A]+\alpha_B[B])^2} P_{\left[N_{B_l}^{A_n}\right]}(\tau) \qquad \text{(S9)}$$

Solving Equation 7 and 8 for with the initial conditions, we have:

$$f_{off}(\tau) = \gamma n_T^2 \frac{\alpha_A[A]\alpha_B[B]}{(1+\alpha_A[A]+\alpha_B[B])^2} exp\left(\gamma n_T^2 \frac{\alpha_A[A]\alpha_B[B]}{(1+\alpha_A[A]+\alpha_B[B])^2}\tau\right) = \gamma_{app} exp(-\gamma_{app}) \qquad \text{(S10)}$$

Then, $\langle\tau_{off}\rangle^{-1}$ represents the rate of product formation for a single nanoparticle:

$$\langle\tau_{off}\rangle^{-1} = \frac{1}{\int_0^\infty \tau f_{off}(\tau)d\tau} = \gamma n_T^2 \frac{\alpha_A[A]\alpha_B[B]}{(1+\alpha_A[A]+\alpha_B[B])^2} = \frac{\gamma_{eff}\alpha_A[A]\alpha_B[B]}{(1+\alpha_A[A]+\alpha_B[B])^2} \qquad \text{(S11)}$$

Where, $\gamma_{eff} = \gamma n_T^2$. In our experiments, the concentration of H_2 is fixed and the [A] can be seen as a constant. From this equation, $\langle\tau_{off}\rangle^{-1}$ should increase initially and then decrease with increasing substrate concentration [B].

Derivation of the distribution of the on-time, f_{on}, and of $\langle\tau_{on}\rangle^{-1}$

The on-time τ_{on} in the single-turnover trajectories spans from product formation to product dissociation, and it is the residence time of a product molecule on the nanoparticle surface after its formation. For product desorption, we considered two parallel desorption reaction pathways: one a substrate-assisted indirect pathway (Ⅱ-Ⅲ) and the other a direct desorption pathway (Ⅳ) (Figure S2):

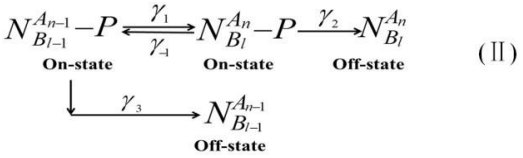

(Ⅱ)

Under the assumption of the mechanism where fast substrate adsorption equilibrium is established at all time, $N_{B_l-1}^{A_{n-1}}$ state will be quickly turned to the $N_{B_l}^{A_n}$ state， as substrate molecular in the solution will quickly bind to an available site to maintain the equilibrium. The conventional kinetic rate equations in concentration terms:

$$\frac{d\left[N_{B_{l-1}}^{A_{n-1}}-P\right]}{d\tau} = -(\gamma_1^0+\gamma_3)\left[N_{B_l-1}^{A_{n-1}} - P\right] + \gamma_{-1}\left[N_{B_l-1}^{A_{n-1}} - P\right] \qquad \text{(S12)}$$

$$\frac{d\left[N_{B_{l-1}}^{A_{n-1}}\right]}{d\tau} = \gamma_1^0\left[N_{B_l-1}^{A_{n-1}} - P\right] - (\gamma_{-1} + \gamma_2)\left[N_{B_l-1}^{A_{n-1}} - P\right] \qquad \text{(S13)}$$

$$\frac{d\left[N_{B_l}^{A_n}\right]}{d\tau} = \gamma_2\left[N_{B_l}^{A_n} - P\right] \qquad \text{(S14)}$$

$$\frac{d\left[N_{B_{l-1}}^{A_{n-1}}\right]}{d\tau} = \gamma_3\left[N_{B_l}^{A_n} - P\right] \qquad \text{(S15)}$$

In the equations $\gamma_1^0 = \gamma_1[A][B]$. Then the concentration terms of nanoparticles were replaced by their probabilities. We obtained:

$$\frac{dP_{N_{B_l}^{A_n}-P}(\tau)}{d\tau} = \gamma_1^0 P_{N_{B_l}^{A_n}-P}(\tau) - (\gamma_{-1}+\gamma_2)P_{N_{B_l}^{A_n}-P}(\tau) \quad \text{(S16)}$$

$$\frac{dP_{N_{B_{l-1}}^{A_{n-1}}-P}(\tau)}{d\tau} = -(\gamma_1^0+\gamma_3)P_{N_{B_{l-1}}^{A_{n-1}}-P}(\tau) + \gamma_{-1}P_{N_{B_l}^{A_n}-P}(\tau) \quad \text{(S17)}$$

$$\frac{dP_{N_{B_l}^{A_n}}(\tau)}{d\tau} = \gamma_2 P_{N_{B_l}^{A_n}-P}(\tau) \quad \text{(S18)}$$

$$\frac{dP_{N_{B_{l-1}}^{A_{n-1}}-P}(\tau)}{d\tau} = \gamma_3 P_{N_{B_{l-1}}^{A_{n-1}}-P} \quad \text{(S19)}$$

In initial conditions for the Equations S16-S19: $P_{N_{B_{l-1}}^{A_{n-1}}}(0) = 1$,

$P_{N_{B_l}^{A_n}}(0) = P_{N_{B_l}^{A_n}-P}(0) = P_{N_{B_{l-1}}^{A_{n-1}}-P}(0) = 0$, and t = 0 is the onset of each on-time τ_{on}, and at any time within τ_{on}: $P_{N_{B_{l-1}}^{A_{n-1}}}(\tau) + P_{N_{B_l}^{A_n}}(\tau) + P_{N_{B_l}^{A_n}-P}(\tau) + P_{N_{B_{l-1}}^{A_{n-1}}-P}(\tau) = 1$

We then consider the probability density $f_{on}(\tau)$ of the on-time τ_{on}. In the two reaction paths, the probability of finding a particular τ is $f_{on}(\tau)\Delta\tau$, which is equal to the sum of the probability for the nanoparticle to switch from the $N_{B_{l-1}}^{A_{n-1}} - P$ states to the $N_{B_l}^{A_n}$ state between τ and $\tau+\Delta\tau$ and the probability from the $N_{B_{l-1}}^{A_{n-1}} - P$ state to the $N_{B_{l-1}}^{A_{n-1}}$ state between τ and $\tau+\Delta\tau$. Then we have

$$f_{on}(\tau) = \frac{dP_{N_{B_{l-1}}^{A_{n-1}}}(\tau)}{d\tau} + \frac{dP_{N_{B_l}^{A_n}}(\tau)}{d\tau} = \gamma_2 P_{N_{B_l}^{A_n}-P}(\tau) + \gamma_3 P_{N_{B_{l-1}}^{A_{n-1}}-P} \quad \text{(S20)}$$

Solving eqs (S16-S19) for $P_{N_{B_l}^{A_n}}(\tau)$ and $P_{N_{B_{l-1}}^{A_{n-1}}-P}(\tau)$ by method of mathematics in the initial conditions, we get

$$f_{on}(\tau) = \frac{1}{2\alpha}\left[Me^{(\alpha+\beta)\tau} + Ne^{(\beta-\alpha)\tau}\right] \quad \text{(S21)}$$

$$\alpha = \sqrt{(\gamma_1[A][B] + \gamma_{-1}+\gamma_2+\gamma_3)^2/4 - (\gamma_1\gamma_2[A][B] + \gamma_{-1}\gamma_3 + \gamma_2\gamma_3)}$$
$$\beta = -(\gamma_1[A][B] + \gamma_{-1}+\gamma_2+\gamma_3)/2$$
$$M = \gamma_1\gamma_2[A][B] + \gamma_3(\alpha+\beta+\gamma_{-1}+\gamma_2)$$
$$N = -\gamma_1\gamma_2[A][B] + \gamma_3(\alpha-\beta-\gamma_{-1}-\gamma_2)$$

At different substrate concentration, $f_{on}(\tau)$ will exhibit different forms.[S3] When the substrate concentration is extremely low and it is without the substrate-assisted desorption pathway, that is $\gamma_1 = \gamma_{-1} = \gamma_2 = 0$. Equation S21 reduces to $f_{on}(\tau) = \gamma_3 e^{-\gamma_3\tau}$, which is a single-exponential decay function with a decay constant γ_3. If [B] is high and the substrate-assisted pathway exists for product desorption, eq S21 will reduce to a single-exponential decay, $f_{on}(\tau) = \gamma_2 e^{-\gamma_2\tau}$.The high substrate concentration here derives the product desorption toward the substrate-assisted pathway, making the direct desorption negligible.

Then $\langle\tau_{on}\rangle^{-1}$, which represents the time-averaged product desorption rate for a single nanoparticle, is

$$\langle\tau_{on}\rangle^{-1} = \frac{1}{\int_0^\infty \tau f_{on}(\tau)d\tau} = \frac{\gamma_2 K[A][B]+\gamma_3}{1+K[A][B]} = \frac{\gamma_2 G[B]+\gamma_3}{1+G[B]} \quad \text{(S22)}$$

Here, $K = \gamma_1/(\gamma_{-1}+\gamma_2)$. The concentration of [A] can be seen as a constant, G = K[A].
Consider the limiting conditions for $\langle\tau_{on}\rangle^{-1}$ When [B]→0,

$$\langle\tau_{on}\rangle^{-1} = \frac{\gamma_2 G[B]+\gamma_3}{1+G[B]} = \gamma_3 \quad \text{(S23)}$$

When [B]→∞,

$$\langle\tau_{on}\rangle^{-1} = \frac{\gamma_2 G[B]+\gamma_3}{1+G[B]} = \gamma_2 \qquad \text{(S24)}$$

To give a physical interpretation of [B] dependence of $\langle\tau_{on}\rangle^{-1}$, when [B] → 0, the tendency forward reaction Ⅲ is extremely low, then the product desorption dominantly takes the direct desorption pathway (reaction Ⅳ) and the reaction rate constant is γ_3. When [B]→∞, the product desorption will dominantly take the substrate-assisted pathway (reaction Ⅲ) and the reaction rate constant is γ_2.

The possible effect of deactivation on the catalysis of Pt nanocatalysts.

The activation of Pt nanoparticle dependent on temperature was determined with 10 nm Resazurin and saturated hydrogen at 35 ^{o}C for about 3 h. And there is no obvious deactivation during the long time reaction process.

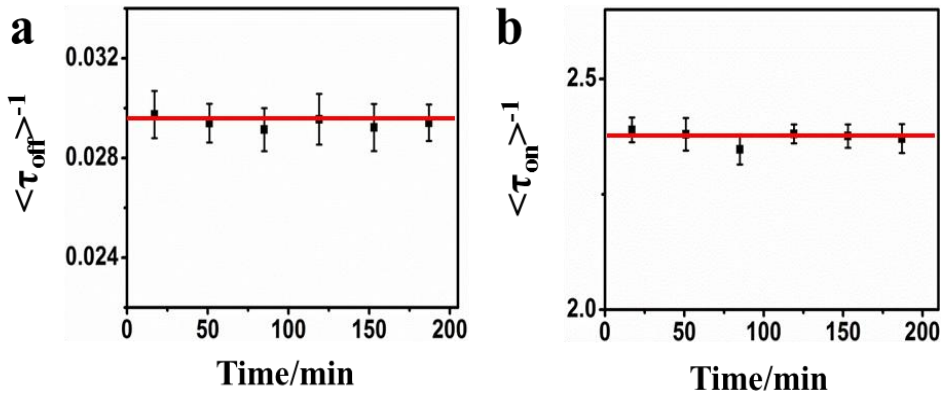

Figure S4. Time dependence of $<\tau_{off}>^{-1}$ (a) and $<\tau_{on}>^{-1}$ (b) from > 90 fluorescence turnover trajectories of Pt nanoparticles with 10 nm Resazurin and saturated hydrogen, error bar is S.E.M.

Distribution of γ_{app}, τ_{off} and τ_{on} of Pt nanoparticles at different temperatures

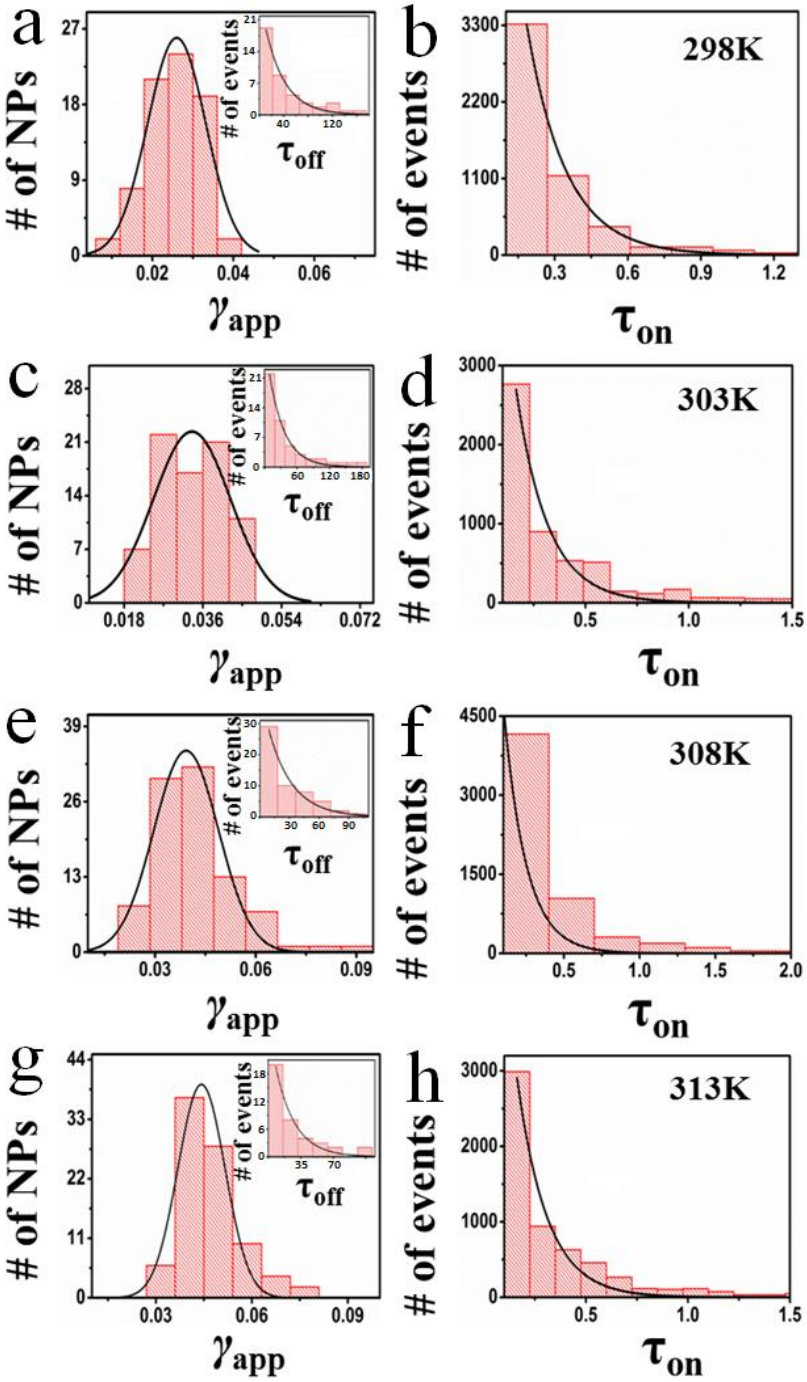

Figure S5. The distribution of γ_{app} of nanoparticles at (a) 25 ^{o}C, (c) 30 ^{o}C, (e) 35 ^{o}C (g)40 ^{o}C with 7 nM resazurin and saturated hydrogen; solid lines are Gaussian fits. Insets: distributions of τ_{off} from a single trajectory; solid line is a single exponential fit with decay constant (a) γ_{app}= 0.031 ±0.003 s^{-1} (c) γ_{app}= 0.035 ± 0.002 s^{-1}, (e) γ_{app}= 0.041 ± 0.004 s^{-1}, (g) γ_{app}= 0.048 ± 0.003 s^{-1}. (b, d, f, h) Distribution of τ_{on} from many trajectories of (b) 25 ^{o}C, (d) 30 ^{o}C, (f) 35 ^{o}C, (h) 40 ^{o}C at the same experimental conditions; solid lines are single-exponential fits and the fitting values are listed in Table 3.

Catalytic dynamic of Pt nanoparticle depending on temperature

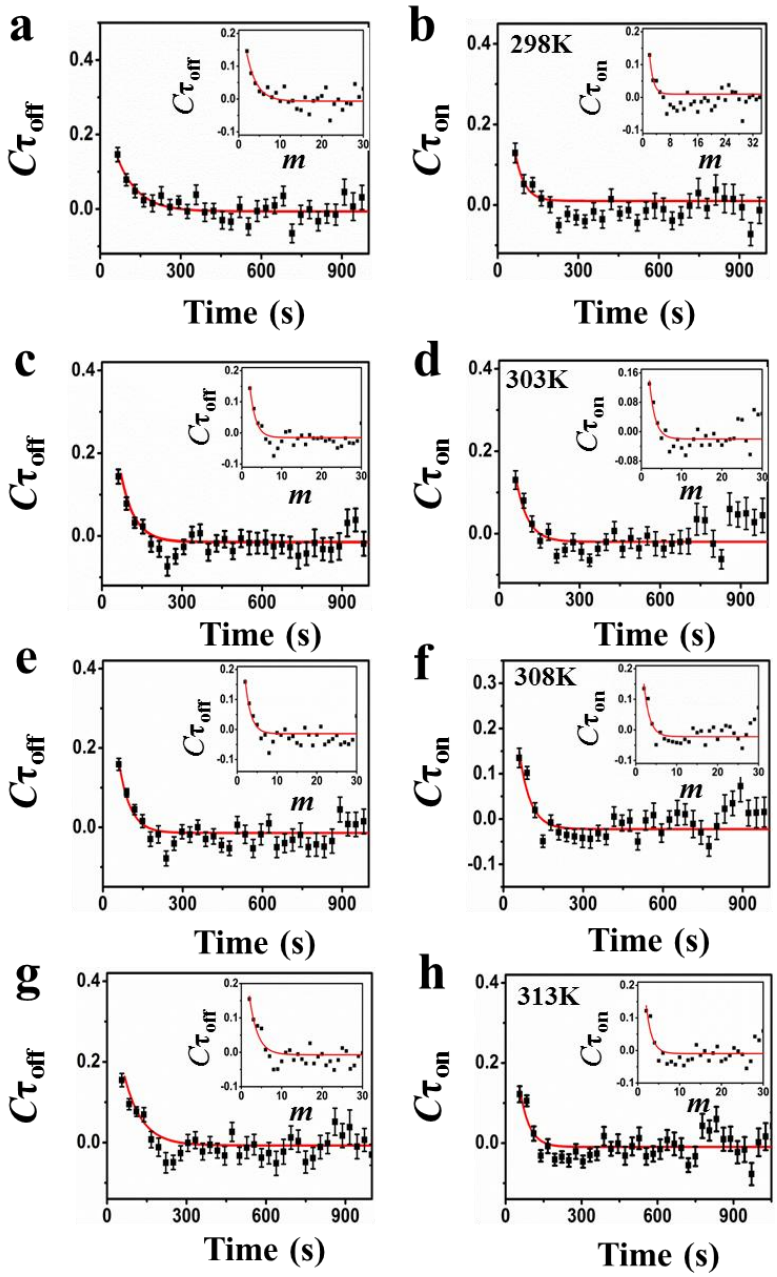

Figure S6. (a, c, e, g) Autocorrelation function $C\tau_{off}(t)$ of the microscopic reaction time τ from turnover trajectories of single Pt nanoparticles with 5nM resazurin and saturated H_2 at (a) 25 ^oC , (c) 30 ^oC, (e) 35 ^oC (g) 40 ^oC. The x-axis was converted from the turnover index *m* to turnover time using the average turnover time of each nanoparticle, and each data is an average from >50 trajectories. Solid line is a single exponential fit and fluctuation correlation times are (a) 47 ± 5 s, (c) 40 ±4 s, (e) 36 ±4 s, (g) 31 ±2 s. Inset: autocorrelation function of the τ_{off} from the turnover trajectory at 25 ^oC, 30 ^oC, 35 ^oC and 40 ^oC, respectively; solid line is a single exponential fit with decay constant of (a) 1.5 ±0.5, (c) 1.3 ± 0.3, (e) 1.2 ± 0.3, (g) 1.1 ± 0 turnovers. (b, d, f, h) Same for τ_{on} process of Pt nanoparticles with 5 nM resazurin at 25^oC, 30 ^oC, 35 ^oC and 40 ^oC, respectively. And fluctuation times are (b) 49 ± 6 s, (d) 44 ±5 s, (f) 38 ±4 s, (h) 36 ±4 s. Data is an average from >50 trajectories. Insert: same as insert a, c, e, g and the decay constants are (b) 1.5 ±0.7, (d) 1.4 ± 0.4, (f) 1.3 ± 0.5, (h) 1.2 ± 0.4 turnovers.

References

S1. Bigall, N. C.; Härtling, T.; Klose, M.; Simon, P.; Eng, L. M.; Eychmuller, A. Monodisperse Platinum Nanospheres with Adjustable Diameters from 10 to100 nm: Synthesis and Distinct Optical Properties. *Nano Lett.* **2008,***8*, 4588-4592.

S2. Han, K. S.; Liu, G.; Zhou, X.; Medina, R. E.; Chen, P. How does a single Pt nanocatalyst behave in two different reactions? A single-molecule study. *Nano Lett.* **2012,***12*, 1253-1259.

S3. Xu, W.; Kong, J. S.; Yeh, Y.-T. E.; Chen, P. Single-molecule nanocatalysis reveals heterogeneous reaction pathways and catalytic dynamics. *Nat. Mater.* **2008**, *7*, 992.

S4. Xu, W.; Shen, H.; Kim, Y. J.; Zhou, X.; Liu, G.; Park, J.; Chen, P. Single-Molecule Electrocatalysis by Single-Walled Carbon Nanotubes. *Nano letters* **2009**, *9*, 3968.